RMetS

Royal Meteorological Society

World drought frequency, duration, and severity for 1951–2010

Jonathan Spinoni,* Gustavo Naumann, Hugo Carrao, Paulo Barbosa and Jürgen Vogt

Joint Research Centre, Institute for Environment and Sustainability, Climate Risk Management Unit, Ispra (VA), Italy

ABSTRACT: In the context of climate change characterized by rising temperature and more extreme precipitation regimes, drought is one of the most relevant natural disasters. This paper presents maps of global drought frequency, duration, and severity for the periods 1951–1970, 1971–1990, and 1991–2010, to give an overview of the respective drought hot spots. Drought frequency is defined as the number of drought events occurred, drought duration as the number of months in drought conditions, and drought severity as the sum of the integral area below zero of each event. Because drought is mainly driven by rainfall deficits, we chose the Standardized Precipitation Index (SPI) as the base indicator to derive drought-related quantities. SPI-12 has been calculated on a monthly basis using a Gamma distribution fitted to a 60-year baseline period (1951–2010). Global grids ($0.5° \times 0.5°$) of the Full Data Reanalysis Version 6.0 dataset provided by the Global Precipitation Climatology Centre (GPCC) have been used as precipitation data input. The regions most exposed to prolonged and severe droughts during 1951–1970 were the Central United States, the Argentinian Pampas, Russia, and Central Australia; during 1971–1990 they were Southern Chile, the Sahel, and Siberia; during 1991–2010 they were the Amazon Forest, the Congo River Basin, Mongolia, North Eastern China, and Borneo. A linear trend analysis between 1951 and 2010 shows a small global increase in each drought component, but drought frequency decreased in the Northern Hemisphere. The increase in drought frequency, duration, and severity is found to be significant in Africa, Eastern Asia, Mediterranean region, and Southern Australia, while the Americas and Russia show a decrease in each drought component.

KEY WORDS   climate change; drought; precipitation; SPI; trends; world

Received 7 June 2013; Revised 21 October 2013; Accepted 23 October 2013

1. Introduction

Drought is a natural hazard related to a prolonged lack of rainfall that leads to a temporary decrease or deficit in natural water availability (Vogt and Somma, 2000). It should not be confused with aridity, which is a permanent climatic feature of a certain region (Wilhite, 1993), or with water scarcity, a situation where the available water resources are insufficient to satisfy long-term average requirements. Droughts have led to widespread societal and environmental impacts and multiple droughts may lead to progressive land degradation and desertification, as it happened following the devastating drought of the Sahel in the late 1960s and the early 1970s (Zeng, 2003). Unlike other disasters, such as floods, tornados, tropical cyclones, earthquakes, or volcanic eruptions, drought is a slowly developing phenomenon as it propagates through the full hydrological cycle and it often shows persistent consequences after its termination (Vogt *et al.*, 2011b).

In general, we can distinguish between four different kinds of droughts (Dracup *et al.*, 1980; Wilhite and Glantz, 1985): meteorological drought, which is caused by a deficit in precipitation with respect to the climatological average for a given period and region; agricultural drought, which is the consequence of a soil moisture deficit leading to a lack of water supply to crops; hydrological drought, which is caused by stream-flow deficits, leading to low water levels in rivers, lakes, or reservoirs; and socio-economic drought, which is linked to the practical consequences of the above-mentioned types of droughts on the supply and demand of some economic goods and services and hence on the life quality of populations. Recently, Mishra and Singh (2010) suggested adding groundwater drought as a fifth category.

Droughts may result in long-term social, economic, and environmental impacts which affect large areas and populations: about half of the Earth's land area is susceptible to drought (Kogan, 1997) and the International Disaster Database (EM-DAT, 2013) recently reported that drought disasters killed more than 11 million people and affected more than 2 billion people from 1900 to 2011. On a global basis, Dai *et al.* (2004) provided evidence for the increasing number of droughts as global warming leads to higher temperatures and enhances dry conditions. Similar conclusions, but with a smaller increase in global drought frequency (DF), were found by Sheffield *et al.* (2012).

In the last decades, drought started to be a more recurrent feature of the European climate that is not

* Correspondence to: J. Spinoni, European Commission - Joint Research Centre, Institute for Environment and Sustainability - Climate Risk Management Unit, TP 280, Via E. Fermi 2749, I-21027 Ispra (VA), Italy. E-mail: jonathan.spinoni@jrc.ec.europa.eu; jonathan.spinoni@gmail.com

restricted to the Mediterranean area as droughts occur both in high and low annual rainfall areas and in any season (Lloyd-Hughes and Saunders, 2002). Moreover, it has been estimated that European droughts caused approximately 100 billion Euros of damage from 1976 to 2006 (Vogt *et al.*, 2011a).

This study deals with meteorological drought: it is based on the analysis of precipitation as rainfall is the leading driver of drought. However, droughts are created by blocking patterns within the atmosphere, favouring subsidence and higher temperatures (and which may divert storm trajectories away from an area, below normal precipitation), antecedent soil moisture conditions, antecedent groundwater (water table) and surface water elevation, evaporation, and advection of high temperature air into a region. The selection of a single drought indicator (SPI) only measures the precipitation input into this process and thereby cannot really said to be a complete description of the entire drought process drought, *per se.*

The principal aim of this study is the construction of global drought frequency, severity, and duration maps related to different periods between 1951 and 2010. These maps highlight the drought hot spots during 1951–1970, 1971–1990, and 1991–2010, providing an overview of areas most hit by drought events in the last 60 years.

The final results provide useful information for climatologists and a wide range of stakeholders interested in the occurrence and the consequences of recurrent droughts. Examples are the European Drought Observatory (EDO, http://edo.jrc.ec.europa.eu), the activities towards a Global Drought Information System (GDIS, Pozzi *et al.* 2013), or the idea of a Global Drylands Observing System (Verstraete *et al.*, 2011), as well as the third edition of the World Atlas of Desertification (WAD; http://wad.jrc.ec.europa.eu).

Section 2 of this paper is dedicated to data and methods, describing the precipitation dataset used to calculate the Standardized Precipitation Index (SPI, McKee *et al.*, 1993), the SPI calculation method, and the definition of the drought-related variables. Section 3 provides the results: global drought frequency, severity, and duration maps are discussed together with derived drought trends and comparisons *versus* the published literature. Section 4 provides the conclusions and gives a brief summary of the results achieved and an outlook on follow-on activities.

2. Data and methods

2.1. Input precipitation data

Precipitation data were obtained from a free global gridded dataset: the Full Data Reanalysis Version 6.0 provided by the Global Precipitation Climatology Centre (GPCC) of the Deutscher Wetterdienst (DWD; Becker *et al.*, 2013). This choice was based on three main reasons: first, it is a spatially interpolated dataset based on the highest number of collected precipitation records; second, it spans from January 1901 to December 2010

and all grid points have no missing data after January 1951; third, this dataset has already been used in many drought-related studies from regional to global scales.

Examples are the analysis of droughts in South Africa (Rouault and Richard, 2003), the drought in the Iberian Peninsula (Garcia-Herrera *et al.*, 2007), different drought indicators in Europe (Pietzsch and Bissolli, 2011), drought variability in Iran (Raziei *et al.*, 2011), the drought of 2010 in the Amazon Forest (Marengo *et al.*, 2011), droughts in the Horn of Africa (Kurnik *et al.*, 2011), historical droughts in Qilian Mountains (Liu *et al.*, 2009), and the study of the relation between droughts and global warming (Dai, 2011).

Version 6.0 is based on the rational merging of data series from rain-gauges built from Global-Telecommunication-System-based data and historic data records, for a world-wide total of more than 67 000 stations that feature record durations of at least 10 years. It contains the monthly totals on regular grids with a spatial resolution of $0.5° × 0.5°$, $1.0° × 1.0°$, and $2.5° × 2.5°$. Although the overall number of input stations is high, it strongly reduced in the last decade both on global and continental basis (Figure 1).

In order to avoid introducing biases due to such a decrease, the spatial and temporal variability of the three products were tested, together with the presence of outliers and spurious signals. The high-resolution monthly product $(0.5° × 0.5°)$ was selected for the analysis, because it passed all the tests and allows better analysing the regional drought patterns. Some problems were found in the regions with fewer data coverage, namely Greenland, Arctic areas, Sahara Desert, Tibetan Plateau, Mexico, and Chile. However, the outliers were extremely rare ($<0.15\%$) and were not used in the computations. If a grid point failed the homogenization test performed with the Multiple Analysis of Series for Homogenization software (MASHv3.02; Szentimrey, 1999), a weighted combination of the precipitation values of the surrounding eight grid points was used instead.

2.2. The Standardized Precipitation Index

The SPI is a statistical monthly indicator that compares the cumulated precipitation during a period of n months with the long-term cumulated rainfall distribution for the same location and accumulation period. It was first introduced by McKee *et al.* (1993) as a measure of the precipitation deficit uniquely based on probability. If computed over short-time periods (up to 3 months), SPI is appropriate for measuring short-term impacts on soil moisture, snowpack, and stream flows of small rivers; SPI related to medium-term cumulated values (3–12 months, i.e. SPI-3 to SPI-12) is appropriate for measuring the impact on stream flow and reservoir storage; SPI for long accumulation periods (12–24 months) is best for assessing long-term processes such as groundwater recharge (McKee *et al.*, 1993).

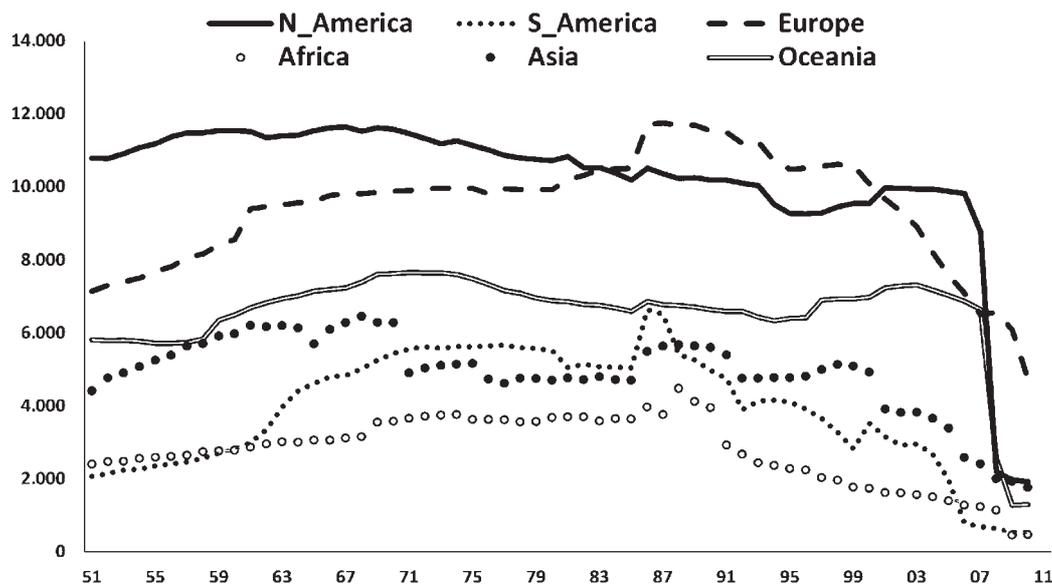SPI was chosen as the basis for computing drought-related components because of a number of reasons.

Figure 1. Number of stations per continent used by GPCC to compute global monthly precipitation grids.

First, it needs only precipitation inputs; second, it is a flexible indicator based on robust underlying probability functions and it has high spatial coherence; third, it is widely used and accepted in drought studies. In general, SPI ranks at the top positions among drought indicators for robustness and reliability (Heim, 2002; Keyantash and Dracup, 2002).

Indeed, SPI has been recommended by the World Meteorological Organization (WMO, 2012) and nowadays SPI is probably the most used drought indicator worldwide: many national meteorological services and drought monitoring centres use it, such as the European Drought Observatory (Vogt *et al.*, 2011a) and the U.S. Drought Monitoring Center (Svoboda *et al.*, 2002).

A long list of applications of SPI can be found in the scientific literature, as it has been used for drought assessments publications on every continent. Examples in Europe are: the work by Lloyd-Hughes and Saunders (2002), for Greece by Tsakiris and Vangelis (2004), and for the Carpathian Area by Spinoni *et al.* (2013); in Asia, e.g. for China by Zhai *et al.* (2010) and for Korea by Min *et al.* (2003); in Africa by Ntale and Gan (2003) and Naumann *et al.* (2012); in Australia by Mpelasoka *et al.* (2008); in Northern America by Agnew (2000) and in South America by Zanvettor and Ravelo (2000) for Argentina. It has also been used for drought forecasting (Cancelliere *et al.*, 2007; Singleton, 2012).

Unfortunately, SPI has some disadvantages: the fitting of the data to the distribution is an approximation and the choice of the theoretical distribution can bias the results; the spatial representativeness of the SPI may be biased by the interpolation method and the data availability; dry regions can be misrepresented owing to the high number of no-rainfall days and the extreme variability in low-rainfall environments; over the entire reference period heavy droughts occur with the same frequency at all locations as a consequence of the standardization.

Before finally choosing SPI, we tested three other indicators as potential candidates for the analysis: the Standardized Precipitation-Evapotranspiration Index (SPEI: Vicente-Serrano *et al.*, 2010), the Palmer Drought Severity Index (PDSI: Palmer, 1965; self-calibrated PDSI: Wells *et al.*, 2004), and the Reconnaissance Drought Index (RDI: Tsakiris *et al.*, 2007). According to our preliminary tests performed at global scale, they proved to have more difficulties than SPI: SPEI can mistake a heat wave for a meteorological drought, RDI can show unrealistic extreme values in areas exposed to seasonal intense precipitation alternated with dry seasons, and PDSI needs too many input variables that are not always available with the same resolution at global scale.

In order to calculate the SPI, the first step relates to the estimation of the parameters for a certain distribution of precipitation sums for the point considered and for the timescale of interest. No single distribution can be optimal for all the grid points (Stagge *et al.*, 2013), but the Gamma distribution proved to be the most robust and consequently is the most frequently used in literature (McKee *et al.*, 1995; Guttman, 1999; Yusof and Hui-Mean, 2012).

The parameters of the Gamma probability density function are used to calculate the cumulative probability distribution of accumulated precipitation for a specific point for the required month and temporal scale. The cumulative probability must be then transformed into a standardized distribution with a zero mean and standard deviation of one (Edwards and McKee, 1997): practically, SPI values are the number of deviations left (negative values refer to a drought event) or right (positive values refer to a wet event) from zero. The magnitude of the departure from the mean gives a probabilistic measure of intensity of the wet or dry event.

Table 1. Classification used for SPI by McKee *et al.* (1993).

SPI value	Class
SPI ≥ 2.0	Extreme wet
$1.5 \leq$ SPI < 2.0	Very wet
$1.0 \leq$ SPI < 1.5	Wet
$-1.0 <$ SPI < 1.0	Normal
$-1.5 <$ SPI ≤ -1.0	Dry
$-2.0 <$ SPI ≤ -1.5	Very dry
SPI ≤ -2.0	Extreme dry

Changing the underlying parameters of the Gamma distribution from one time period to another will affect the SPI values and if different time lengths of precipitation records are involved in the SPI calculations, the outputs may be geographically inconsistent. The longer the record used for SPI calculations, the more reliable the SPI values. It is therefore recommended using at least 30 years of data (Wu *et al.*, 2005). More details about the theoretical background of SPI can be found in, e.g. Lloyd-Hughes and Saunders (2002).

SPI-12 was calculated using the cumulated rainfall from the global precipitation grids provided by GPCC. All the precipitation data from 1951 to 2010 were used to fit the distributions.

In Table 1 we show the SPI classes as suggested by McKee *et al.* (1993). We followed the original classification, though different classifications based on percentiles (Agnew, 2000) and on Markov chains (Paulo *et al.*, 2005) have been proposed recently.

2.3. Defining a drought event and drought frequency, severity, and duration

The SPI-12 was selected to construct the global drought frequency, severity, and duration maps presented in this paper. The underlying reason is that a medium-term accumulation period (12 months) is more suitable to depict the various world precipitation regimes than shorter (SPI-3, SPI-6) or longer periods (SPI-24, SPI-48), which might be too sensitive to extremes or miss relevant drought events. However, the drought statistics discussed in this study are not much affected by the choice of SPI-12 in spite of SPI-6 or SPI-24. In fact, we found comparable drought patterns on spatial basis, both on global and continental scale, using different aggregation periods (6, 12, and 24 months).

The monthly SPI-12 values from 1951 to 2010 were used to define drought events according to the methodology of McKee *et al.* (1993): a drought starts in the month when SPI falls below -1 and it ends when SPI returns to positive values, in this analysis for at least two consecutive months. Similar truncation thresholds have been adopted by Mishra *et al.* (2009), but many others can be chosen, see Panu and Sharma (2002) for a review.

To define the drought-related variables we adapted the run model described by Yevjevich (1967). Once a drought event has been determined with its start and end month, its duration and severity were then assigned. The duration of a drought event is equal to the number of months between its start (included) and end month (not included); the severity is the absolute value of the integral area between the SPI line and the horizontal axis (SPI $= 0$) from the start to the end month of the drought. Severity should not be mistaken for intensity, which is usually referred to the lowest SPI value of the drought event.

Drought frequency (DF), total drought duration (TDD), and total drought severity (TDS) were then computed for every grid point and every 10- and 20-year interval between 1951 and 2010. In the maps, DF is expressed as the number of events in the considered period, TDD and TDS represent the sum of the durations and severities of the drought events occurred in the considered period and they are expressed in number of months and in a dimensionless drought severity score, respectively.

2.4. Excluding very arid and extremely cold areas from the drought maps

It was assumed that dealing with drought concepts in extremely dry and cold regions would be physically meaningless. In order to exclude these areas from computations by means of an objective methodology, a combination of conditions derived from three different indicators was used. A similar land-masking strategy was used by Ziese *et al.* (2013) for drought monitoring based on a special indicator derived from the merging of SPI and SPEI.

First, areas where one or more months show more than 25% zero values of cumulated precipitation were excluded. This avoids computing biased SPI-12 records based on Gamma distributions constructed over an insufficient number of values.

Second, the arid areas have been excluded using the FAO Aridity Index (AI; UNEP, 1992), computed as the ratio between the annual cumulated precipitation and the annual cumulated evapotranspiration (ET). For simplicity, ET was replaced by potential evapotranspiration (PET). One single AI value, related to the average of sixty annual AI values from 1951 to 2010, was assigned to each grid point. According to the AI classification, global areas are divided into: humid (AI > 0.75), sub-humid ($0.65 <$ AI ≤ 0.75), dry ($0.5 <$ AI ≤ 0.65), semi-arid ($0.2 <$ AI ≤ 0.5), arid ($0.05 <$ AI ≤ 0.2), hyper-arid ($0.03 <$ AI ≤ 0.05), and desert (AI ≤ 0.03). Areas with AI ≤ 0.05 were excluded from the analysis.

Third, the cold areas have been excluded using the annual PET: if the average PET between 1951 and 2010 was smaller than 365 mm, the drought variables for the corresponding grid points were not computed. Moreover, Antarctica was labelled as cold land and cut off from the maps. We obtained PET, also used to compute AI, from the CRUTS v3.20 dataset (Climate Research Unit Time Series; Mitchell and Jones, 2005) of the University of East Anglia.

The total emerged lands of the Earth sum up to 148.94×10^6 km^2 (National Geographic Society, 2010). The drought maps take into account 100.35×10^6 km^2
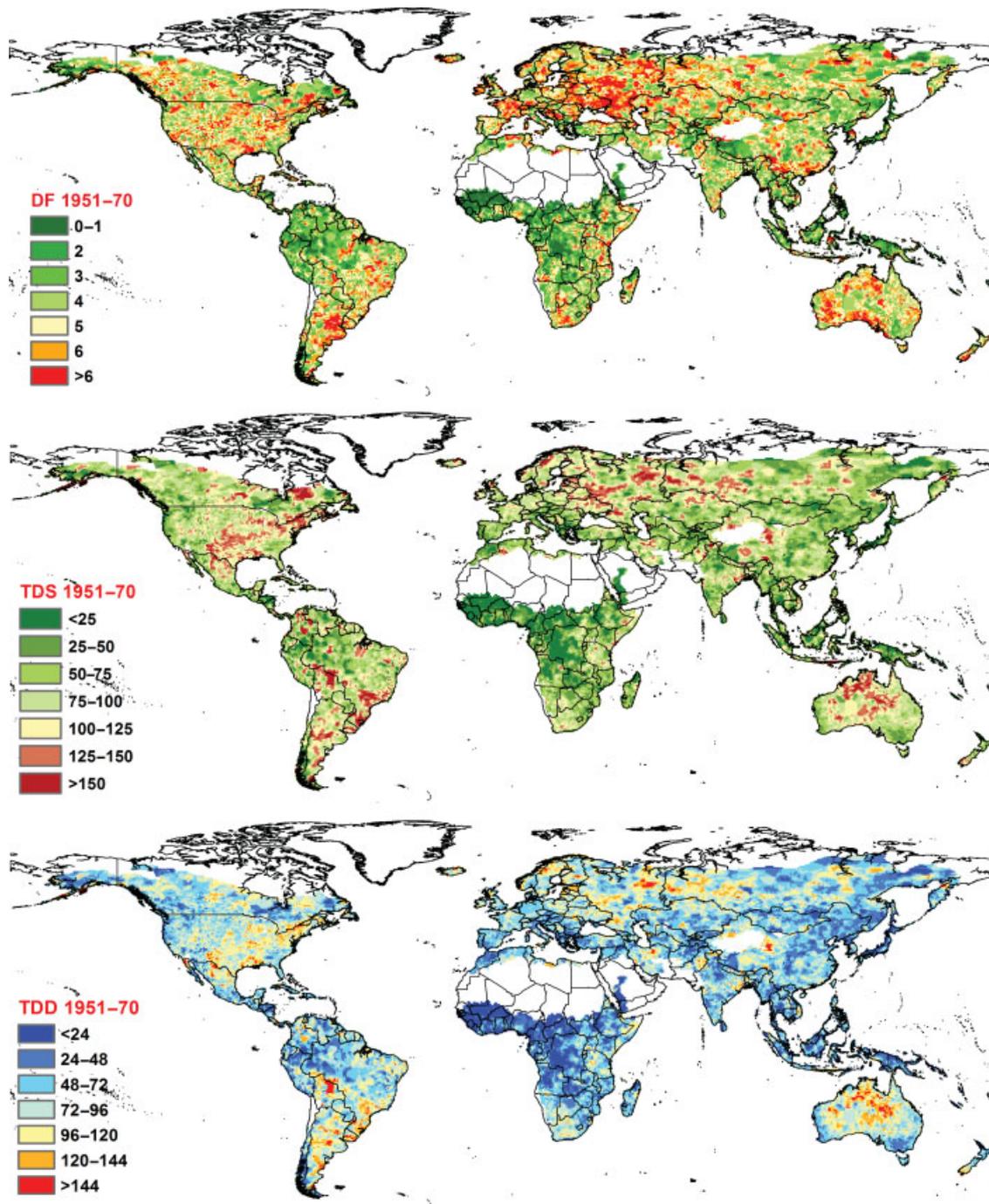
Figure 2. Drought frequency (top), total drought severity (centre), and total drought duration (bottom) maps for 1951–1970.

which corresponds to 67% of the total emerged lands or to 74% if Antarctica (about 14×10^6 km^2) is not considered. The excluded regions are shown as white areas in Figures 2–7.

3. Results and discussion

3.1. Drought frequency, duration, and severity maps for 1951–1970, 1971–1990, and 1991–2010

Figures 2–4 show the DF, TDS, and TDD maps for each of the three selected periods (1951–1970, 1971–1990,

and 1991–2010). To provide a complete picture of the hot spots of the last six decades, we preferred splitting into three 20-year intervals, because two 30-year periods may give insufficient information on the variability. Drought severity and duration maps show similar spatial patterns, as they are connected, while drought frequency maps show different features, depending on the period and the continent.

During 1951–1970 (Figure 2), the drought hot spots according to drought severity and duration were located in the Central and North-Eastern United States, Bolivia, the Argentinian Pampas and Southern Brazil, European
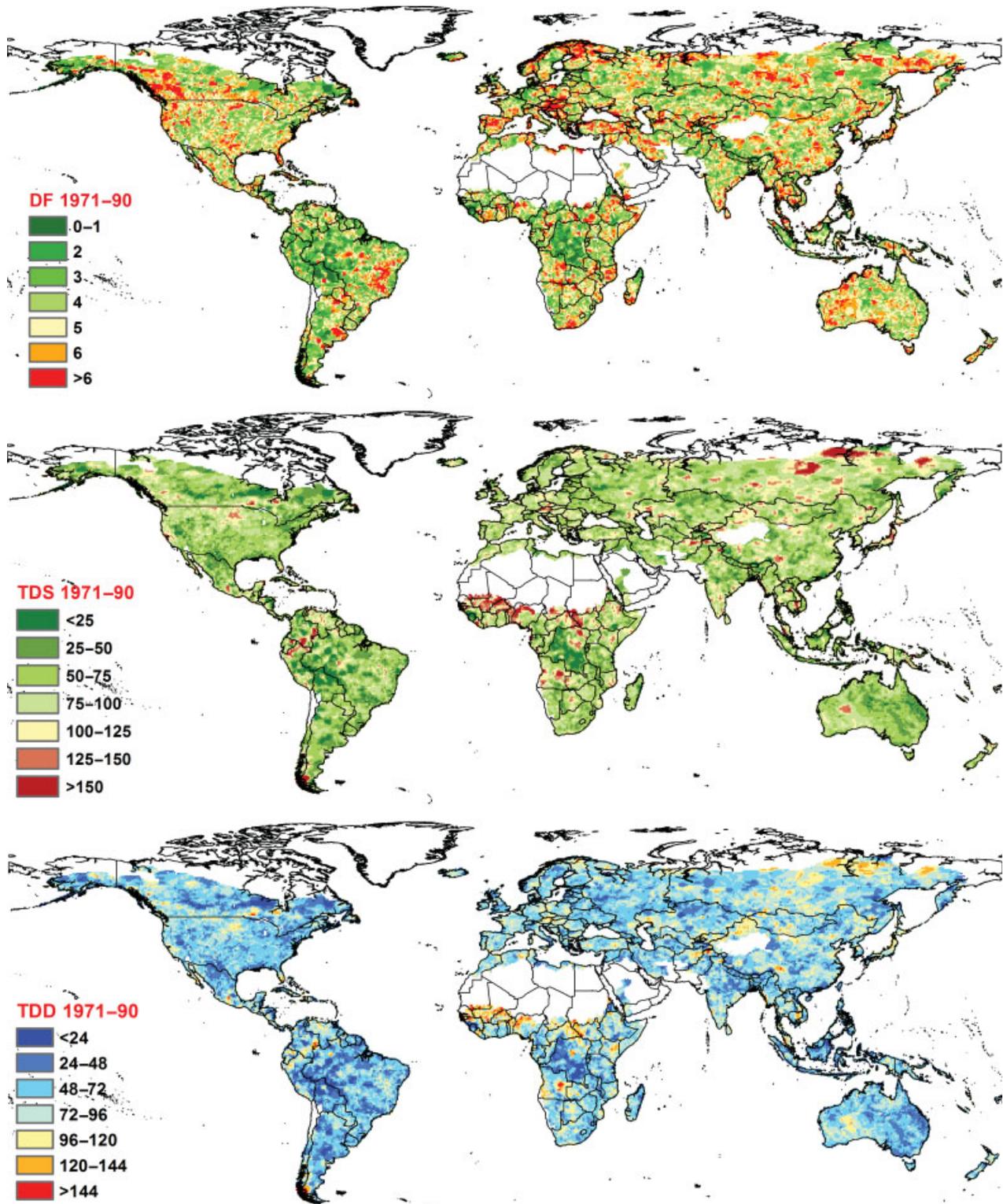
Figure 3. Drought frequency (top), total drought severity (centre), and total drought duration (bottom) maps for 1971–1990.

Russia, and Central and Northern Australia. High drought frequencies can be seen in France, South-Eastern China, South Africa, and South-Western Australia.

There are many publications dealing with relevant droughts in these areas during 1951–1970: Andreadis *et al.* (2005) and Sheffield *et al.* (2009) reported the great drought of 1952 in the Central United States and the

drought of 1963 in the North-Eastern United States; Scian and Donnari (1997) and Sheffield *et al.* (2009) accounted for the droughts in Argentina in the 1950s and in South America in 1963 and 1968; Sheffield and Wood (2007) reported also the droughts in Australia in 1957, 1961, and 1965 and the prolonged effects of the drought and famine in the late 1940s and the early 1950s in Russia;
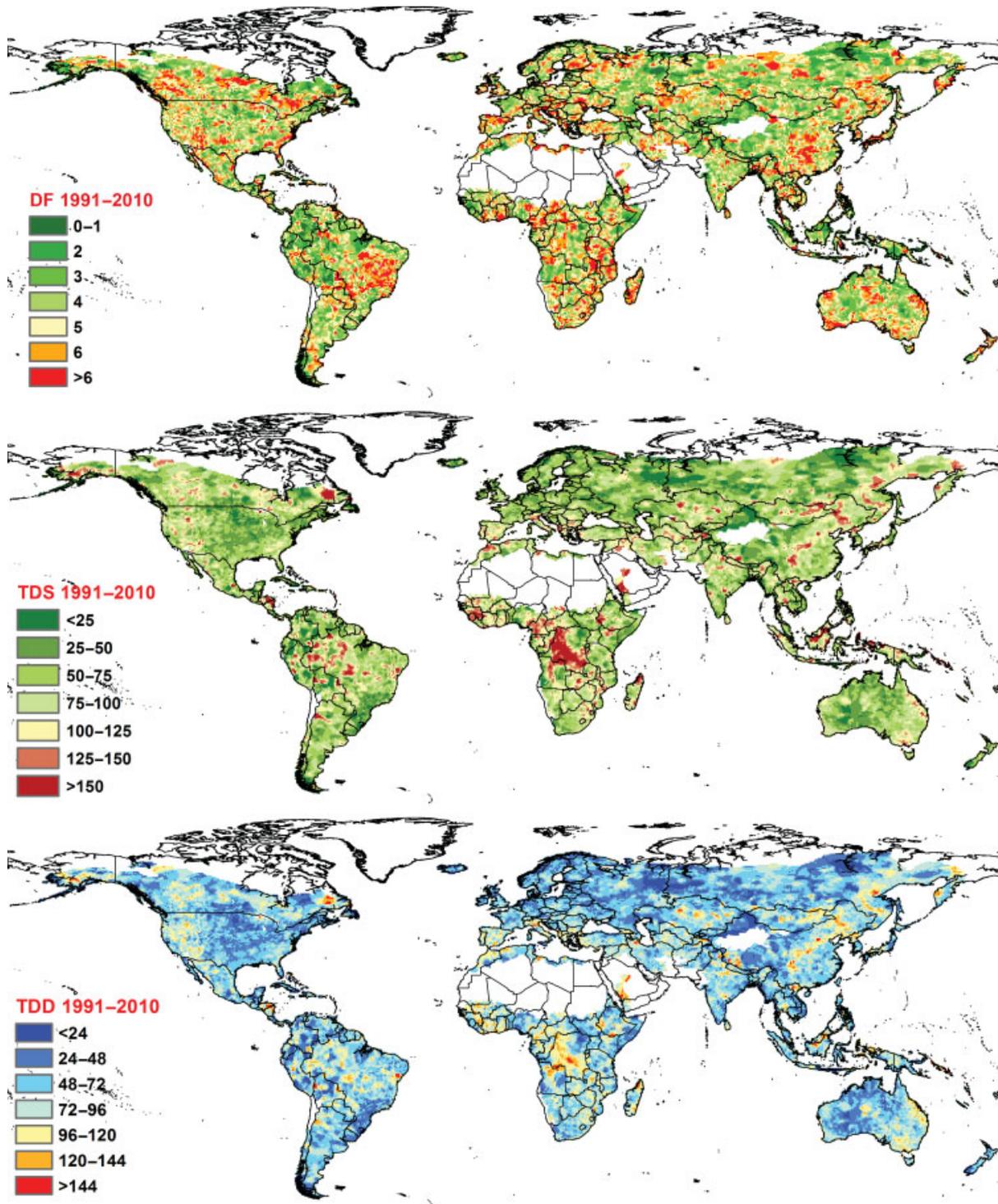
Figure 4. Drought frequency (top), total drought severity (centre), and total drought duration (bottom) maps for 1991–2010.

Li *et al.* (2003) reported the droughts in China in the late 1950s, which contributed also to the Chinese famine in the years 1958–1961.

During 1971–1990 (Figure 3), the drought hot spots were less prominent in many regions. However, significant events were located in Colombia, Southern Chile, the African territories between the Tropic of Cancer and the Equator (in particular, the Sahel region, Ethiopia, and South Sudan), Angola, and Russian Siberia. At

the same time, frequent but less severe drought events occurred in Western Canada, Florida, Spain, Scandinavia, the Balkans, the Horn of Africa, South Africa, Myanmar, and Western Australia.

The devastating Sahel drought in the 1970s was widely reported in literature (Charney, 1975; Zeng, 2003) and it was one of the main reasons that fostered the creation of the United Nations Convention to Combat Desertification (UNCCD; Vogt *et al.*, 2011a); the recurrent droughts that
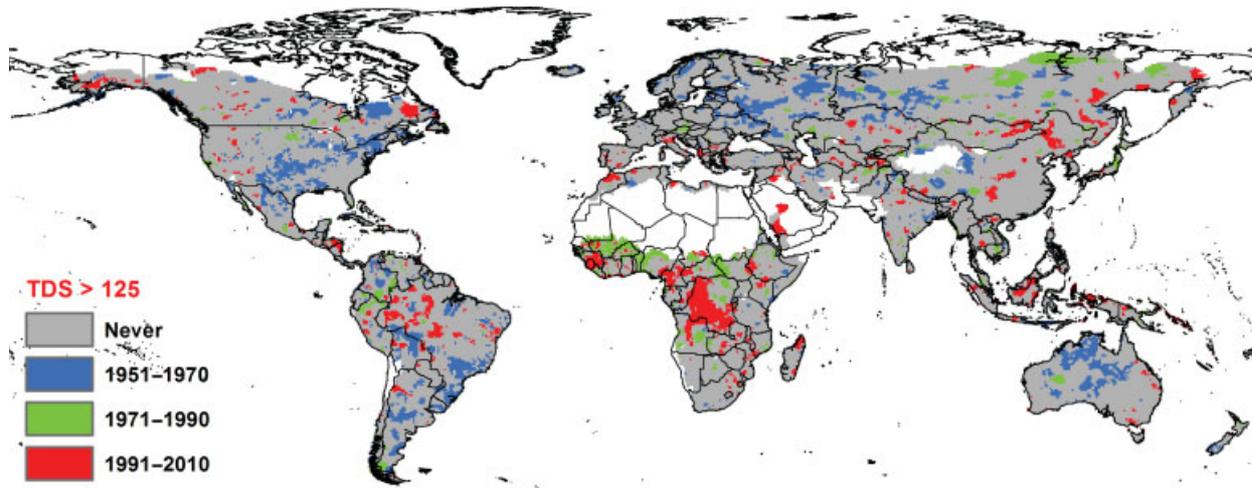
Figure 5. Drought hot spots in the periods 1951–1970, 1971–1990, and 1991–2010.

hit Ethiopia and Sudan in the periods 1973, 1982–1984, 1987, and 1990 were mentioned by Henricksen and Durkin (1986) and the Emergency Events Database (EM-DAT) of the World Health Organization (WHO) Collaborating Centre for Research on the Epidemiology of Disasters (CRED) reported that the droughts between 1983 and 1985 resulted in more than half a million deaths in Ethiopia and Sudan (EM-DAT, 2013); a heavy drought in easternmost Russia in 1972 was reported by Meshcherskaya and Blazhevich (1997); the high frequency and less severe of droughts in Argentina were described by Sheffield and Wood (2007); the drought of 1982 in Western Australia was reported by Nicholls (2004).

During 1991–2010 (Figure 4), the drought hot spots were located in Amazonia, Guinea and the Gulf of Guinea, the Congo River basin, Borneo, Papua, the Yangtze River basin, and Mongolia. In addition, frequent droughts occurred in Canada, Texas, and the Atlantic Coast of the United States, Brazil, the Mediterranean region, Central-Eastern Africa and Madagascar, China, Asian Russia, and along the Australian coasts.

The drought of 2002 in the United States was described by Andreadis *et al.* (2005), the one of 2001–2002 in Canada by Wheaton *et al.* (2008). Marengo *et al.* (2008, 2011) focused on the drought of 2005 and 2010 in Amazonia. The drought that followed the heat wave of summer 2003 in Europe was studied, e.g. by Rebetez *et al.* (2006); furthermore, Lloyd-Hughes and Saunders (2002), van der Schrier *et al.* (2006), and Hoerling *et al.* (2012) affirmed that the Mediterranean area and Central Europe have been hit by frequent droughts in the last decades. Heavy droughts further hit the Democratic Republic of Congo in the 1990s (Laraque *et al.*, 2001; Dai *et al.*, 2004), and Mali, Mauritania, and Niger in the 2000s (EM-DAT, 2013). Asia was hit by many relevant drought events in the last two decades: China in 1994 (EM-DAT estimates total damages of 13.76 billion dollars owing to the reduced rice production), in 1997, and in 2002 (Zhang *et al.*, 2013), the Tibetan

Plateau in 1997–2000 (Sheffield *et al.*, 2009), and India in 2002 (Prabhakar and Shaw, 2008) with about 300 million people affected (EM-DAT, 2013). In the late 1990s a drought coupled with forest fires hit Borneo (Van Nieuwstadt and Sheil, 2005) and the worst drought of its history hit Papua (McVicar and Bierwirth, 2001); finally, the so-called Millennium Drought hit Australia from 1995 to 2012 (Nicholls, 2004; Horridge *et al.*, 2005).

Although the number of stations used to compute the GPCC's precipitation grids strongly decreased in the last decade, the drought variables were also computed for the period 2001–2010, but the maps are not shown here. Compared to the 20-year periods discussed above, the last decade shows a number of pronounced hot spots, both with respect to duration and severity: the Central and Western United States, Nicaragua and Honduras, Guinea, Gulf of Guinea, Angola, Tajikistan, India, Mongolia, North-Eastern China, and Western Coast and New South Wales in Australia. In particular, North-Eastern China and the Gulf of Guinea in Africa have been the areas most hit by severe and long drought events during 2001–2010.

To summarize, the drought hot spots of the different periods are shown in Figure 5, which shows all the regions with a TDS larger than 125 (the 90th percentile in the global distribution of TDS with all the values of the three 20-year periods) in the periods 1951–1970, 1971–1990, and 1991–2010. The most affected areas were China and India, Southern and Central Australia, the Sahel region and Central Africa, Amazonia, the Central United States, Russia, and Southern Europe.

3.2. Inter-decadal drought variability

Drought trends are often derived from long-term series of PDSI, while trends based on standardized indicators such as SPI or SPEI are less frequently reported (Lloyd-Hughes and Saunders, 2002; Vicente-Serrano *et al.*, 2010).
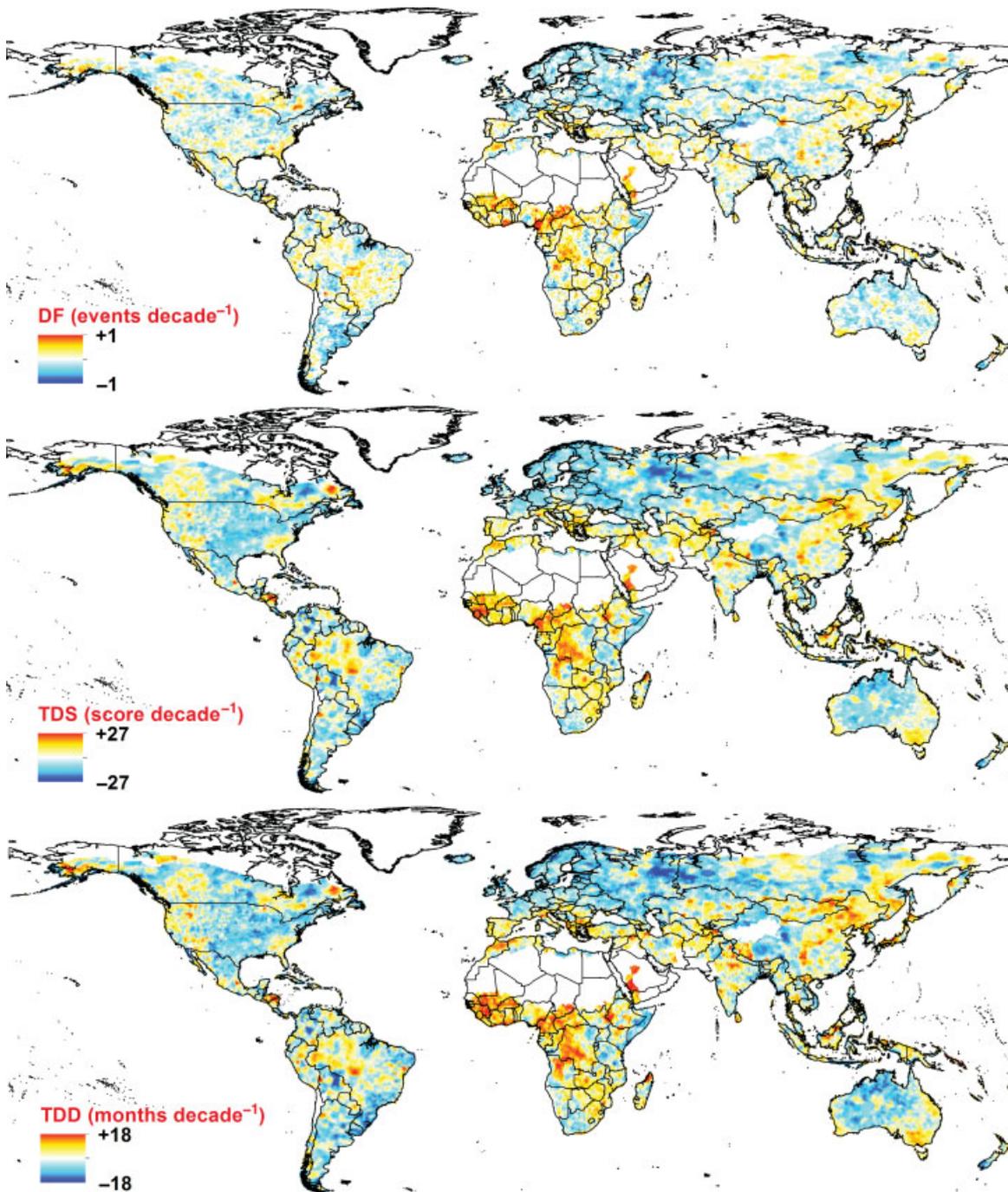
Figure 6. Linear trends for drought frequency, severity, and duration in the years 1951–2010.

We studied the inter-decadal variability of droughts in the last 60 years by computing DF, TDS, and TDD for each 10-year period during 1951 to 2010. We performed a linear trend analysis over the six periods and the statistical significance of each trend has been tested with the Student's *T*-test (Gosset, 1908) with a confidence level of 95%. This methodology has a limitation: the trends are based on 10-year values, so they have been computed using six points only. Still they provide a first identification of potential hot spot areas.

In Figures 6 and 7, the DF trends are shown in events per decade, while TDS and TDD trends are shown in

drought scores per decade and in months per decade, respectively. In general, regions that experienced big drought events in the 1950s such as Russia, the United States, and the Argentinian Pampas often show negative trends, while regions where big drought events occurred in the last 10 years, such as the Gulf of Guinea, are often characterized by positive drought trends.

To provide global statistics, we consider a trend as relevant if it is significant at 95% and it is larger (smaller) than 0.05 events decade^{-1} for DF, than 15 score decade^{-1} for TDS, and than 12 months decade^{-1} for TDS. In this way, we excluded the grid points with trend values so
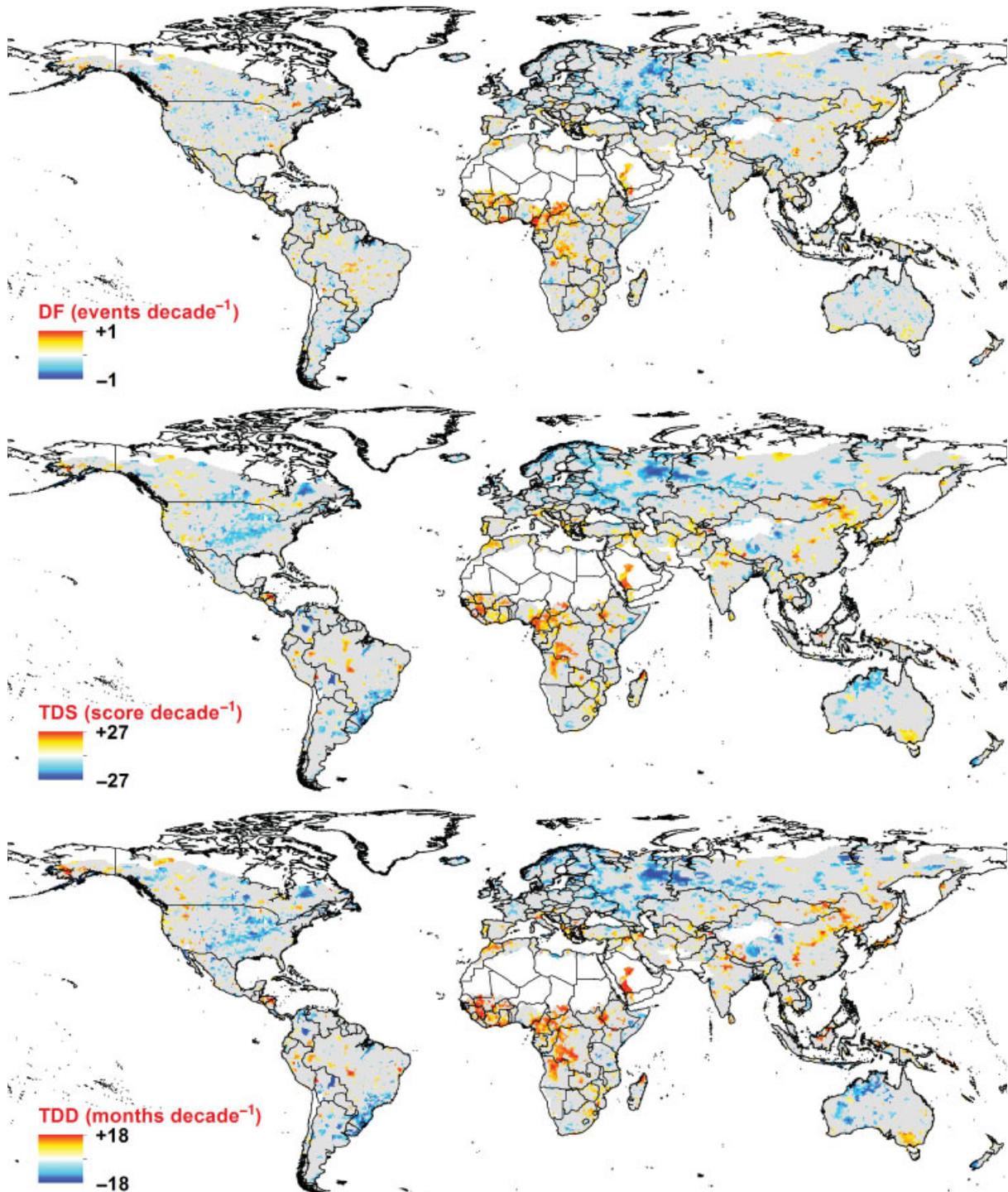
Figure 7. Linear trends for drought frequency, severity, and duration in the years 1951–2010. In grey areas the trends are not significant at 95% level.

small that they are physically meaningless. Globally, each drought component shows a small increase, though DF slightly decreased in Northern Hemisphere. If we split the entire period into two intervals and we base the analysis on 5-year frames, a small decrease in each drought component occurred during 1951–1980, followed by an opposite increase during 1981–2010.

On continental basis, drought trends (Figure 6) follow the precipitation patterns of the last decades (IPCC,

2007); in particular, DF, TDS, and TDD show a decrease in the Americas (except the Western United States, Alberta, and Amazonia), Russia, and Northern Australia, *versus* an increase in Africa, Asia (except Siberia), Mediterranean region, and southern Australia. The most important significant increases (Figure 7) can be observed in tropical and subtropical Africa (Sahel and Congo) and in North-Eastern China, while the most important decreases in the Central United States, European

Russia, and in the border areas between Argentina and Brazil.

3.3. Comparisons of our drought maps and trends with recently published studies

Dai *et al.* (2004) computed drought trends based on the PDSI and Thornthwaite's (TH) model for PET (Thornthwaite, 1948): regarding 1950–2002 they found that DF and intensity increased most in Canada, the Sahel, the Mediterranean area, Mongolia, and North-Eastern China; on a spatial basis their results are very similar to ours.

However, if the actual temperature rise is used in the models, the positive trends are much larger than if a constant temperature is used. Recently, Dai (2011) and Sheffield *et al.* (2012) discussed drought trends of the last 60 years: they showed that different computation techniques result in different evaluations of the global drought trends.

In particular, drought indicators such as the PDSI and the self-calibrated PDSI (sc-PDSI) can be biased by the methodology chosen to calculate PET: the Thornthwaite's and the Penman-Monteith's models (PM; Allen *et al.*, 1998) account for temperature in different ways, and the former may amplify PET at high temperatures.

Sheffield *et al.* (2012) computed drought trends for 1950–2008 using a different indicator (sc-PDSI with PM model) and different datasets with respect to this study, but they reported only a small global increase in DF and duration in the last 60 years, thus our results agree with their findings. Similar agreement has been found with the results reported by Burke *et al.* (2006).

Furthermore, Sheffield *et al.* (2012) found similar spatial patterns in drought trends as compared with the maps presented in this study: a significant increase in the Sahel, Mongolia and North Eastern China, Alberta (Canada), and South-Eastern Australia, versus a significant decrease in the Central United States, Argentina, Central and North-Western Australia. Only one relevant difference can be noticed: drought increased in Central and Northern Europe for Sheffield *et al.* (2012). Similar spatial patterns to ours have been found by Damberg (2013) also, with one major exception only: we reported of increasing drought trends in the Sahel region, while Damberg (2013) did not.

We may conclude that, on a spatial basis and regarding the statistical significance of the reported drought trends, the maps presented in this study are more similar to the maps presented by Sheffield *et al.* (2012) based on the sc-PDSI with PM model, than the ones based on the PDSI or sc-PDSI with TH model presented in the same paper.

4. Conclusions

This paper provides a simple and complete picture of the occurrence and characteristics of meteorological droughts based on a single precipitation indicator (SPI-12). Drought frequency, severity, and duration maps were produced for 1951–1970, 1971–1990, and 1991–2010 on a $0.5° × 0.5°$ global grid. The resulting 20-year drought climatologies represent an overview of drought hot spots in the last 60 years. The locations of the hot spots for each 20-year period are visually summarized in Figure 4.

Drought frequency, severity, and duration trends were found to be consistent with the results found by Dai (2011) and Sheffield *et al.* (2012) by means of sc-PDSI. Our results have been obtained with a different methodology: they are based on SPI, which is much simpler to be computed than PDSI and sc-PDSI, as they need more input variables that are not easily available at global scale. Globally, we document a small increase in drought components, which regards in particular the last decades, though the 1950s proved to be the decade most hit by severe and prolonged drought events. On continental basis, the Americas and Russia are subject to a significant decrease in drought variables, while the Mediterranean, Central Africa, Amazonia, North-Eastern China, and Southern Australia are subject to significant increases. Drought severity and duration seem to be subject to a steeper increase than frequency in Africa and Eastern Asia.

In the future, we plan compiling global and continental drought climatologies based on a multi-indicator approach. We also plan coupling drought indicators with soil information and aridity indicators, to evaluate to which degree a temporary slowly developing phenomenon such as drought can lead to permanent land degradation and even desertification.

Acknowledgements

References

Agnew CT. 2000. Using the SPI to identify drought. *Drought Netw. News* **12**: 6–12.

Allen RG, Pereira LS, Raes D, Smith M. 1998. Crop evapotranspiration: Guidelines for computing crop water requirements. *Irrigation and Drainage Paper No 56*, UN-FAO, Rome.

Andreadis KM, Clark EA, Wood AW, Hamlet AF, Lettenmaier DP. 2005. Twentieth-century drought in the conterminous United States. *J. Hydrometeorol.* **6**(6): 985–1001.

Becker A, Finger P, Meyer-Christoffer A, Rudolf B, Schamm K, Schneider U, Ziese M. 2013. A decription of the global land-surface precipitation data products of the Global Precipitation Climatology Centre with sample applications including centennial (trend) analysis from 1901-present. *Earth Syst. Sci. Data* **5**: 71–99.

Burke EJ, Brown SJ, Christidis N. 2006. Modeling the recent evolution of global drought and projections for the twenty-first century with the Hadley Centre Climate Model. *J. Hydrometeorol.* **7**: 1113–1125.

Cancelliere A, Di Mauro G, Bonaccorso B, Rossi G. 2007. Drought forecasting using the standardized precipitation index. *Water Resour. Manage.* **21**(5): 801–819.

Charney JG. 1975. Dynamics of deserts and drought in the Sahel. *Q. J. R. Meteorol. Soc.* **101**: 193–202.

Dai A. 2011. Drought under global warming: a review. *WIREs: Clim. Change* **2**(1): 45–65.

Dai A, Trenberth KE, Qian T. 2004. A global dataset of Palmer Drought Severity Index for 1870–2002: relationship with soil moisture and effects of surface warming. *J. Hydrometeorol.* **5**(6): 1117–1130.

Damberg L. 2013. Analysis of Trends and Patterns of Droughts Using Satellite Data and Climate Model Simulations. *Avd för Teknisk Vattenresurslära, TVVRYY/500n, ISSN 1101–9824*, http://www.lunduniversity.lu.se/o.o.i.s?id=24923&postid=3458772

Dracup JA, Lee KS, Paulson EG Jr. 1980. On the definition of droughts. *Water Resour. Res.* **16**(2): 297–302.

Edwards DC, McKee TB. 1997. *Characteristics of 20th century drought in the United States at multiple timescales*. Colorado State University: Fort Collins. Climatology Report No. 97-2.

EM-DAT. 2013, http://www.emdat.be/disaster-list.

Garcia-Herrera R, Hernández E, Barriopedro D, Paredes D, Trigo RM, Trigo IF, Mendes MA. 2007. The outstanding 2004/05 drought in the Iberian Peninsula: associated atmospheric circulation. *J. Hydrometeorol.* **8**(3): 483–498.

Gosset WS. 1908. The probable error of a mean. *Biometrika* **6**(1): 1–25.

Guttman NB. 1999. Accepting the standardized precipitation index: a calculation algorithm. *J. Am. Water Resour. Assoc.* **35**(2): 311–322.

Heim RR Jr. 2002. A review of twentieth-century drought indices used in the United States. *Bull. Am. Meteorol. Soc.* **83**(8): 1149–1165.

Henricksen BL, Durkin JW. 1986. Growing period and drought early warning in Africa using satellite data. *Int. J. Remote Sens.* **7**(11): 1583–1608.

Hoerling M, Eischeid J, Perlwitz J, Quan X, Zhang T, Pegion P. 2012. On the increased frequency of Mediterranean drought. *J. Clim.* **25**(6): 2146–2161.

Horridge M, Madden J, Wittwer G. 2005. The impact of the 2002–2003 drought on Australia. *J. Policy Model.* **27**(3): 285–308.

IPCC. 2007. *Climate Change 2007-The Physical Science Basis: Working Group I Contribution to the Fourth Assessment Report of the IPCC*, Vol. **4**, Solomon S (ed). Cambridge University Press: Cambridge and New York, NY.

Keyantash J, Dracup JA. 2002. The quantification of drought: an evaluation of drought indices. *Bull. Am. Meteorol. Soc.* **83**(8): 1167–1180.

Kogan FN. 1997. Global drought watch from space. *Bull. Am. Meteorol. Soc.* **78**(4): 621–636.

Kurnik B, Barbosa P, Vogt J. 2011. Testing two different precipitation datasets to compute the standardized precipitation index over the Horn of Africa. *Int. J. Remote Sens.* **32**(21): 5947–5964.

Laraque A, Mahé G, Orange D, Marieu B. 2001. Spatiotemporal variations in hydrological regimes within Central Africa during the XXth century. *J. Hydrol.* **245**(1): 104–117.

Li MS, Li S, Li YH. 2003. Studies on drought in the past 50 years in China. *Chin. J. Agrometeorol.* **1**: 002.

Liu W, Gou X, Yang M, Zhang Y, Fang K, Yang T, Jin L. 2009. Drought reconstruction in the Qilian Mountains over the last two centuries and its implications for large-scale moisture patterns. *Adv. Atmos. Sci.* **26**(4): 621–629.

Lloyd-Hughes B, Saunders MA. 2002. A drought climatology for Europe. *Int. J. Climatol.* **22**(13): 1571–1592.

Marengo JA, Nobre CA, Tomasella J, Oyama MD, De Oliveira GS, De Oliveira R, Camargo H, Alves LM, Brown IF. 2008. The drought of Amazonia in 2005. *J. Clim.* **21**(3): 495–516.

Marengo JA, Tomasella J, Alves LM, Soares WR, Rodriguez DA. 2011. The drought of 2010 in the context of historical droughts in the Amazon region. *Geophys. Res. Lett.* **38**(12): L12703.

McKee TB, Doeskin NJ, Kleist J. 1993. The relationship of drought frequency and duration to time scales. In *Proceedings of the 8th Conference on Applied Climatology*. American Meteorological Society: Boston, MA; 179–184.

McKee TB, Doeskin NJ, Kleist J. 1995. *Proceedings of the 9th Conference on Applied Climatology*. American Meteorological Society: Boston, MA; 233–236.

McVicar TR, Bierwirth PN. 2001. Rapidly assessing the 1997 drought in Papua New Guinea using composite AVHRR imagery. *Int J Remote Sens* **22**(11): 2109–2128.

Meshcherskaya AV, Blazhevich VG. 1997. The drought and excessive moisture indices in a historical perspective in the principal grain-producing regions of the former Soviet Union. *J. Clim.* **10**(10): 2670–2682.

Min SK, Kwon WT, Park E, Choi Y. 2003. Spatial and temporal comparisons of droughts over Korea with East Asia. *Int. J. Climatol.* **23**(2): 223–233.

Mishra AK, Singh VP. 2010. A review of drought concepts. *J. Hydrol.* **391**(1): 202–216.

Mishra AK, Singh VP, Desai VR. 2009. Drought characterization: a probabilistic approach. *Stoch. Environ. Res. Risk Assess.* **23**(1): 41–55.

Mitchell TD, Jones PD. 2005. An improved method of constructing a database of monthly climate observations and associated high-resolution grids. *Int. J. Climatol.* **25**(6): 693–712.

Mpelasoka F, Hennessy K, Jones R, Bates B. 2008. Comparison of suitable drought indices for climate change impacts assessment over Australia towards resource management. *Int. J. Climatol.* **28**(10): 1283–1292.

National Geographic Societyed. 2010. *National Geographic Atlas of the World*, 9th edn. National Geographic Society ISBN-10: 1426206348, ISBN-13: 978–1426206344: Washington, DC.

Naumann G, Barbosa P, Carrao H, Singleton A, Vogt J. 2012. Monitoring drought conditions and their uncertainties in Africa using TRMM data. *J. Appl. Meteorol. Climatol.* **51**(10): 1867–1874.

Nicholls N. 2004. The changing nature of Australian droughts. *Clim. Change* **63**(3): 323–336.

Ntale HK, Gan TY. 2003. Drought indices and their application to East Africa. *Int. J. Climatol.* **23**(11): 1335–1357.

Palmer WC, 1965. Meteorologic drought. *U.S. Weather Bureau Research Paper 45*, 58.

Panu US, Sharma TC. 2002. Challenges in drought research: some perspectives and future directions. *Hydrolog. Sci. J.* **47**(S1): S19–S30.

Paulo AA, Ferreira E, Coelho C, Pereira LS. 2005. Drought class transition analysis through Markov and loglinear models, an approach to early warning. *Agric. Water Manage.* **77**(1): 59–81.

Pietzsch S, Bissolli P. 2011. A modified drought index for WMO RA VI. *Adv. Sci. Res.* **6**: 275–279.

Pozzi W, Sheffield J, Stefanski R, Cripe D, Pulwarty R, Vogt J, Heim R, Brewer MJ, Svoboda M, Westerhoff R, van Dijk A, Lloyd-Hughes B, Pappenberger F, Werner M, Dutra E, Wetterhall F, Wagner W, Schubert S, Mo K, Nicholson M, Bettio L, Nuñez L, van Beek R, Bierkens M, Goncalves LG, Zell de Mattos JG, Lawford R. 2013. Toward global drought early warning capability. Expanding International Cooperation for the Development of a Framework for Monitoring and Forecasting. *Bulletin of the American Meteorological Society (BAMS)*, BAMS-D-11-00176, http://dx.doi.org/10.1175/BAMS-D-11-00176

Prabhakar SVRK, Shaw R. 2008. Climate change adaptation implications for drought risk mitigation: a perspective for India. *Clim. Change* **88**(2): 113–130.

Raziei T, Bordi I, Pereira LS. 2011. An application of GPCC and NCEP/NCAR datasets for drought variability analysis in Iran. *Water Resour Manage.* **25**(4): 1075–1086.

Rebetez M, Mayer H, Dupont O, Schindler D, Gartner K, Kropp JP, Menzel A. 2006. Heat and drought 2003 in Europe: a climate synthesis. *Ann. For. Sci.* **63**(6): 569–577.

Rouault M, Richard Y. 2003. Intensity and spatial extension of drought in South Africa at different time scales. *Water SA* **29**(4): 489–500.

Scian B, Donnari M. 1997. Retrospective analysis of the Palmer Drought Severity Index in the semi-arid Pampas region, Argentina. *Int. J. Climatol.* **17**(3): 313–322.

Sheffield J, Wood EF. 2007. Characteristics of global and regional drought, 1950–2000: Analysis of soil moisture data from off-line simulation of the terrestrial hydrologic cycle. *J. Geophys.Res.: Atmospheres (1984–2012)* **112**(D17115): 1–21.

Sheffield J, Andreadis KM, Wood EF, Lettenmaier DP. 2009. Global and continental drought in the second half of the twentieth century: severity-area-duration analysis and temporal variability of large-scale events. *J. Clim.* **22**(8): 1962–1981.

Sheffield J, Wood EF, Roderick ML. 2012. Little change in global drought over the past 60 years. *Nature* **491**(7424): 435–438.

Singleton A. 2012. Forecasting drought in Europe with the Standardized Precipitation Index. *JRC Scientific and Technical Report*, EUR 25254 EN, 68, DOI: 10.2788/16459.

Spinoni J, Antofie T, Barbosa P, Bihari Z, Lakatos M, Szalai S, Szentimrey S, Vogt J. 2013. An overview of drought events in the Carpathian Region in 1961–2010. *Adv. Sci. Res.* **10**: 21–32.

Stagge J, Tallaksen L, Gudmundsson L, van Loon A, Stahl K. 2013. Pan-European comparison of candidate distributions for climatological drought indices, SPI and SPEI. *Geophys. Res. (Abstracts)* **15**: EGU2013–9329.

Svoboda M, Lecomte D, Hayes M, Heim R, Gleason K, Angel J, Rippey B, Tinker R, Palecki M, Stooksbury D, Miskus D, Stephens S. 2002. The drought monitor. *Bull. Am. Meteorol. Soc.* **83**: 1181–1190.

Szentimrey T. 1999. Multiple analysis of series for homogenization (MASH). In *Proceedings of the Second Seminar for Homogenization of Surface Climatological Data*, 27–46.

Thornthwaite CW. 1948. An approach toward a rational classification of climate. *Geograph. Rev.* **38**(1): 55–94.

Tsakiris G, Vangelis H. 2004. Towards a drought watch system based on spatial SPI. *Water Resour. Manage.* **18**(1): 1–12.

Tsakiris G, Pangalou D, Vangelis H. 2007. Regional drought assessment based on the Reconnaissance Drought Index (RDI). *Water Resour. Manage.* **21**(5): 821–833.

UNEP. 1992. *World Atlas of Desertification*, Middleton NJ, Thomas DSG (eds). Edward Arnold: Sevenoaks, UK.

Van der Schrier G, Briffa KR, Jones PD, Osborn TJ. 2006. Summer moisture variability across Europe. *J. Clim.* **19**(12): 2818–2834.

Van Nieuwstadt MG, Sheil D. 2005. Drought, fire and tree survival in a Borneo rain forest, East Kalimantan, Indonesia. *J. Ecol.* **93**(1): 191–201.

Verstraete MM, Hutchinson CF, Grainger A, Stafford Smith M, Scholes RJ, Reynolds JF, Barbosa P, Leon A, Mbow C. 2011. Towards a global drylands observing system: observational requirements and institutional solutions. *Land Degrad. Dev.* **22**(2): 198–213.

Vicente-Serrano SM, Beguería S, López-Moreno JI. 2010. A multi-scalar drought index sensitive to global warming: the standardized precipitation evapotranspiration index. *J. Clim.* **23**(7): 1696–1718.

Vogt JV, Somma F (eds). 2000. *Drought and Drought Mitigation in Europe*. Kluwer Academic Publishers: Dordrecht, The Netherlands; 336.

Vogt JV, Barbosa P, Hofer B, Magni D, De Jager A, Singleton A, Horion S, Sepulcre G, Micale F, Sokolova E, Calcagni L, Marioni M, Antofie TE. 2011a. Developing a European Drought Observatory for Monitoring, Assessing and Forecasting Droughts across the European Continent. In *AGU Fall Meeting Abstracts 1*, NH24A-07.

Vogt JV, Safriel U, Von Maltitz G, Sokona Y, Zougmore R, Bastin G, Hill J. 2011b. Monitoring and assessment of land degradation and desertification: towards new conceptual and integrated approaches. *Land Degrad. Dev.* **22**(2): 150–165.

Wells N, Goddard S, Hayes MJ. 2004. A self-calibrating Palmer drought severity index. *J. Clim.* **17**(12): 2335–2351.

Wheaton E, Kulshreshtha S, Wittrock V, Koshida G. 2008. Dry times: hard lessons from the Canadian drought of 2001 and 2002. *Can Geogr* **52**(2): 241–262.

Wilhite DA. 1993. *Drought Assessment, Management, and Planning: Theory and Case Studies*. Kluwer Academic Publishers: Boston, MA; 293.

Wilhite DA, Glantz MH. 1985. Understanding: the drought phenomenon: the role of definitions. *Water Int.* **10**(3): 111–120.

WMO. 2012. Standardized Precipitation Index User Guide (M. Svoboda, M. Hayes and D. Wood). *WMO-No.1090*, Geneva.

Wu H, Hayes MJ, Wilhite DA, Svoboda MD. 2005. The effect of the length of record on the standardized precipitation index calculation. *Int. J. Climatol.* **25**(4): 505–520.

Yevjevich VM. 1967. An objective approach to definitions and investigations of continental hydrologic droughts. *Hydrology Paper No. 23*, Colorado State University, Fort Collins, 1967.

Yusof F, Hui-Mean F. 2012. Use of statistical distribution for drought analysis. *Appl. Math. Sci.* **6**(21): 1031–1051.

Zanvettor R, Ravelo A. 2000. Using the SPI to monitor the 1999–2000 Drought in Northeastern Argentina. *Drought Netw. News* **12**(4): 4.

Zeng N. 2003. Drought in the Sahel. *Science* **302**(5647): 999–1000.

Zhai J, Su B, Krysanova V, Vetter T, Gao C, Jiang T. 2010. Spatial variation and trends in PDSI and SPI indices and their relation to streamflow in 10 large regions of China. *J. Clim.* **23**(3): 649–663.

Zhang M, He J, Wang B, Wang S, Li S, Liu W, Ma X. 2013. Extreme drought changes in Southwest China from 1960 to 2009. *J. Geograph. Sci.* **23**(1): 3–16.

Ziese M, Schneider U, Meyer-Christoffer A, Finger P, Schamm K, Becker A, Rudolf B. 2013. A combined drought index from the Global Precipitation Climatology Centre (GPCC). *Geophys. Res. (Abstracts)* **15**: EGU2013–4158.